

Article

# A Comparison of the Effect of Activator Cations (Sodium and Potassium) on the Fresh and Hardened Properties of Mine Tailing-Slag Binders

Sahil Surehali , Aswathy Simon , Rijul Kanth Ramasamy and Narayanan Neithalath \* 

School of Sustainable Engineering and Built Environment, Arizona State University, Tempe, AZ 85287, USA; ssurehal@asu.edu (S.S.); asimon9@asu.edu (A.S.)

\* Correspondence: narayanan.neithalath@asu.edu

**Abstract:** This study develops alkali-activated mine tailing (MT)-based binders containing MT as the major source material and slag (S) as a minor additive, using alkaline activators containing sodium or potassium as the cationic species. The influence of the cationic species (Na or K), slag content, alkalinity (expressed using the activator silica modulus,  $M_s$ ), and alkali oxide-to-powder ratio,  $n$ , on the setting behavior, paste rheology, early-age reaction kinetics, and compressive strength development are discussed. The effects of using solid activators are also considered. Changes in  $M_s$  values have a stronger impact on setting times compared to  $n$  values, underscoring the significant role of silicate species from the activator in the initial reaction mechanisms. The type of cation and physical state of the activator (in the case of K-Si-activated systems) are found to determine the dissolution rate and mobility of ionic species in the system, resulting in significant differences in the early age reaction mechanisms (e.g., K-based activators show  $>2\times$  enhancement in early heat release as compared to Na-based activators) of the alkali-activated binders prepared using the same activator parameters. The difference in the viscosities of the activator solutions strongly influences the rheological characteristics of the activated systems. MT-based binders with 28-day compressive strengths ranging from 10 to 35 MPa, which are suitable for several structural/non-structural applications, are attained. The strong dependence of the compressive strength development on the alkali activation parameters and slag content in the system presents an opportunity to develop sustainable binders, with MT as their major constituent, to provide twin benefits of recycling MT wastes and mitigating the environmental impacts associated with traditional ordinary Portland cement-based binder systems.

**Keywords:** mine tailings; slag; alkali activation; reaction kinetics; compressive strength; rheology



**Citation:** Surehali, S.; Simon, A.; Ramasamy, R.K.; Neithalath, N. A Comparison of the Effect of Activator Cations (Sodium and Potassium) on the Fresh and Hardened Properties of Mine Tailing-Slag Binders. *Constr. Mater.* **2023**, *3*, 389–404. <https://doi.org/10.3390/constrmater3040025>

Received: 3 September 2023

Revised: 20 October 2023

Accepted: 23 October 2023

Published: 27 October 2023



**Copyright:** © 2023 by the authors. Licensee MDPI, Basel, Switzerland. This article is an open access article distributed under the terms and conditions of the Creative Commons Attribution (CC BY) license (<https://creativecommons.org/licenses/by/4.0/>).

## 1. Introduction

Mine tailings (MT) are the waste materials left behind after extracting valuable metals or components from minerals and ores during mining operations [1]. The environmental concerns accompanying the enormous amount of MT wastes produced globally (~5–7 billion tons [2,3]) are further aggravated by the high ratio of tailings to valuable metals/components [4,5] and the difficulties in effective waste management practices in the mining sector [6,7]. The conventional practice of disposing of tailings in tailing dams carries with it the risk of polluting water bodies in case the tailing dams fail or discharge untreated waste [8], and the accumulation of toxic constituents in the ecosystem [9–11] that can contaminate food crops, water sources, and the air, leading to significant health hazards [12–14]. Hence, it is essential to devise sustainable waste management strategies to mitigate the risks associated with MT.

A growing trend in the sustainable disposal of MT involves their recycling in various applications including construction materials, fertilizers, glasses and ceramics, and automobile catalytic converters [15,16]. Recent studies have explored the feasibility of incorporating MT into conventional concretes, as well as novel cementing systems such as

inorganic polymers [17–19]. Since MT is primarily composed of silica, alumina, and calcium oxide, similar to that in several building materials [20,21], they have been considered potential candidates for inclusion in construction products [22–24]. However, their low reactivity presents a challenge to use them as an independent binder constituent [3,25]. To enhance the reactivity of MT and create binding systems comparable to those of ordinary Portland cement (OPC)-based systems, several studies augment MT with Ca-containing additives (such as slag) [3,25]. Although effective, this approach reduces the amount of MT in the binder, consequently lowering the recycling efficiency. Researchers have also opted for mechanical pretreatment [26,27] and thermal pretreatment [28,29] to enhance the reactivity of MT for geopolymerization applications. However, both these methods have their limitations. For instance, the energy requirements for dry and wet grinding in mechanical activation have significant implications [30]. Moreover, the effect of mechanical pretreatment on the compressive strength of the final geopolymer is less obvious than that of adding supplementary cementing materials [25].

The presence of alumina and silica in MT presents a possibility that alkali activation of MT can enhance their reactivities and produce more sustainable end products. The overall process is similar to the alkali activation of common aluminosilicate precursors such as fly ash or slag, which is a commonly expounded strategy to produce sustainable binders with properties that are similar or superior to those of traditional cementitious binders [31–33]. Furthermore, the formation of hydration products in alkali-activated slag systems is reported to proceed adequately under moist curing [34]. The curing temperature is less significant than the effects of activator concentration and type in these systems [35]. Since the energy implications of moist curing are much more favorable than those of heat curing, alkali activation of MT becomes more favorable. The precursor composition, alkalinity of the activator solution, and mixture design parameters including the liquid-to-solid ratio and the amount of reactivity enhancers (e.g., slag) significantly influence the fresh and later-age properties of the alkali-activated binders [36–39]. Additionally, the type of the alkali cation and the amounts of alkali oxide and silica present in the system also are reported to exert significant influence on the kinetics of the chemical reaction, the composition of the reaction products formed, and the final binder properties [40,41].

In this paper, efforts are made to develop alkali-activated MT-based binders comprising MT as the main constituent and slag as a minor additive to enhance the overall reactivity of the binder ingredients to attain desirable fresh and hardened properties. The focus is on the influence of the activator cation type (Na or K) and the physical state of the activator (liquid or solid) for different levels of total alkalinity provided by the activator (defined as the ratio of alkali oxide to the total source material content, referred to as  $n$ ), and the molar ratio of silica-to-alkali oxide in the activator ( $M_s$ ). Liquid sodium silicate (waterglass), liquid potassium silicate, and solid potassium silicate are used as the three primary activating agents, along with sodium or potassium hydroxide, to provide the desired alkalinity levels. The influence of the aforementioned parameters on (a) setting time, (b) rheological parameters (yield stress and plastic viscosity), (c) early-age hydration kinetics, and (d) compressive strength as a function of curing time (3, 7, 14, and 28 days) are discussed in detail in this paper. This study is expected to provide guidelines for the development of sustainable alkali-activated binders with MT as a major constituent, thereby allowing for the valorization of MT. Furthermore, the use of MT that contributes to cement reduction leads to reductions in CO<sub>2</sub> emissions, as well.

## 2. Experimental Program

### 2.1. Materials

Mine tailings (MT) obtained from a copper mine, provided by Freeport McMoRan Inc. (FMI), were used as the primary binding material. The tailings were obtained in a slurry form. They were dewatered, oven-dried at 80 °C for 24 h, and crushed into a fine powder before being used in the paste and mortar mixtures. Ground granulated blast furnace slag conforming to ASTM C 989 was used to replace 20% and 30% by mass of

MT in the binder system, ensuring that the tailings remained the major component of the binders. The chemical compositions of the binder (weight%) constituents, as obtained using X-ray fluorescence (XRF), are summarized in Table 1. The copper MT does not contain any detectable amounts of Ca but has a combined ( $\text{SiO}_2 + \text{Al}_2\text{O}_3 + \text{Fe}_2\text{O}_3$ ) > 85%, meeting the chemical requirements of fly ash as per ASTM C 618. The specific gravities of MT and slag were measured to be 2.76 and 2.92, respectively, using a gas pycnometer in accordance with ASTM D 5550. The Blaine fineness of the MT and slag were determined to be  $898 \text{ cm}^2/\text{g}$ , and  $3950 \text{ cm}^2/\text{g}$ , respectively, using a Blaine Air Permeability Apparatus conforming to ASTM C 204. The particle size distribution of the binder ingredients, determined using a laser particle size analyzer, is shown in Figure 1. The median particle sizes ( $d_{50}$ ) were  $38.63 \text{ }\mu\text{m}$ , and  $12.33 \text{ }\mu\text{m}$  for the MT and slag, respectively. This study used three different activating agents to activate the binders: liquid sodium silicate (waterglass), liquid potassium silicate, and solid potassium silicate. The as-obtained Na–Si solution had a solid content of 42.6% and a silica modulus (molar  $\text{SiO}_2$ -to- $\text{M}_2\text{O}$  ratio) or  $M_s$  of 1.60. The liquid K–Si had a solid content of 39.2% and  $M_s$  of 2.10, and the solid K–Si had a solid content of 99.8% and  $M_s$  of 1.60. Sodium hydroxide (NaOH) or potassium hydroxide (KOH) was added to the Na–Si or K–Si activators to reduce their  $M_s$  values to 1.0 and 1.5, as these values were shown to result in efficient activation elsewhere [42].

**Table 1.** Chemical composition of the binder ingredients.

Binder Ingredients	Chemical Composition								
	SiO <sub>2</sub> (%)	Al <sub>2</sub> O <sub>3</sub> (%)	SO <sub>3</sub> (%)	Fe <sub>x</sub> O <sub>y</sub> (%)	SnO (%)	MnO (%)	TiO <sub>2</sub> (%)	Sb <sub>2</sub> O <sub>3</sub> (%)	P <sub>2</sub> O <sub>5</sub> (%)
Mine tailings #	64.2	19.95	1.94	8.26	1.35	0.81	0.48	2.49	0.15
					MgO (%)	Na <sub>2</sub> O (%)	K <sub>2</sub> O (%)	CaO (%)	LOI* (%)
GGBFS	39.4	8.49	2.83	0.37	12.05	0.27	0.80	35.53	1.31

\*—Loss on ignition; #—Traces of oxides of Zr, Mo, and Zn were also detected in mine tailings.

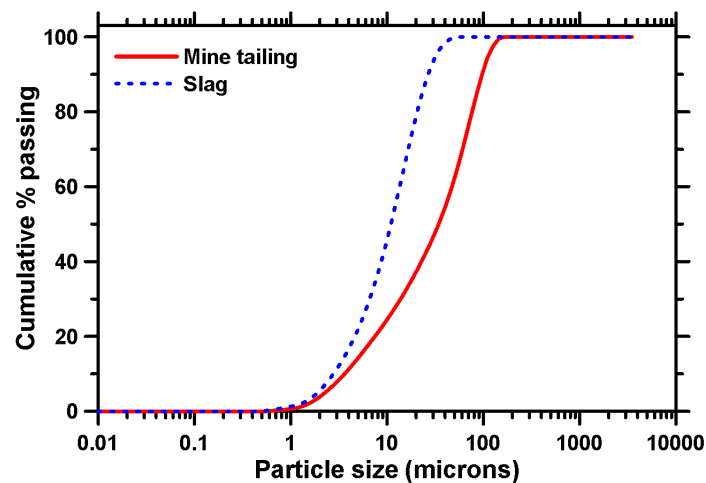


**Figure 1.** Particle size distribution curves for MT and slag.

2.2. Mixture Proportions

As mentioned earlier, slag was used to replace 20% and 30% by mass of MT to develop MT–slag (S) blends. The activator solutions were proportioned based on the following two parameters:  $\text{M}_2\text{O}$ -to-binder (where M is the alkali cation, Na or K) ratio ( $n$ ) and the silica modulus (molar  $\text{SiO}_2$ -to- $\text{M}_2\text{O}$  ratio) ( $M_s$ ) [37]. The activator solution, comprising silicate (Na or K), hydroxide (NaOH or KOH), and water, was proportioned to have  $n$  values of 0.05 and 0.075 and  $M_s$  values of 1.0 and 1.5 [34]. For all the Na and K silicates, NaOH or KOH was added to bring the activator  $M_s$  to 1.0 and 1.50. A water-to-binder ( $w/b$ ) ratio in the range of 0.35 to 0.45 (mass-based) has been shown to result in sufficient workability for alkali-activated slag systems, based on our previous work [39]. Therefore, a  $w/b$  ratio of

0.35 was selected for use in this study after the initial trials. Note that the water consists of the liquid portion of the activator and the additional water required to obtain the desired  $w/b$  (mass-based) ratio. Table 2 summarizes the amounts of activating agents required for 1000 g of binder (MT + slag) for an  $n$  value of 0.05 and the different  $M_s$  values used in this study. The mortar mixtures prepared for compressive strength tests comprised 50% by volume of river sand; 50 mm-sized cubes were moist cured in a chamber at  $23 \pm 2 \text{ }^\circ\text{C}$  and  $>98\%$  RH, and tested at four different ages.

**Table 2.** Amounts of activator agents for 1000 g of binder (MT + slag).

Activator Agent	Liquid Na–Si		Liquid K–Si		Solid K–Si	
	$M_s$	$M_s$	$M_s$	$M_s$	$M_s$	$M_s$
Na/K silicate (g)	190.73	286.09	188.29	282.43	81.41	122.12
NaOH/KOH (g)	24.19	4.03	31.21	17.02	22.34	3.72
Water (g)	235.08	184.88	230.50	175.54	346.25	349.16

### 2.3. Test Methods

The setting times of the pastes were determined using the Vicat needle method in accordance with ASTM C 191. Isothermal calorimetry experiments were carried out for 48 h at a temperature of  $25 \text{ }^\circ\text{C}$  in accordance with ASTM C 1679. The activator solutions were prepared separately and allowed to cool down to ambient temperature. The activator solution was then added to the binder, and the mixture was mixed and placed in the calorimeter. The time between mixing and placing in the calorimeter was around 1 min. The compressive strengths of the selected binders were determined in accordance with ASTM C 109; the 50 mm cubes were moist cured in a chamber at  $23 \pm 2 \text{ }^\circ\text{C}$  and  $>98\%$  RH, and tested at four different ages (3, 7, 14, and 28 days). At least three specimens from each mixture were tested for strength.

The rheological properties of the paste were evaluated using TA Instruments’ AR 2000EX rotational rheometer with a vane geometry, which eliminates issues with slip in rheological measurements, as reported in another study [43]. All the experiments were carried out with the setup maintained at  $25 \pm 0.1 \text{ }^\circ\text{C}$  temperature. Approximately 40 mL of paste was placed in the rheometer geometry using a disposable syringe. The time between adding the mixing activator solution and beginning the rheological experiment was  $<5$  min. A shear rate ramp study (strain-controlled), consisting of a pre-shear phase and a ramp-up and ramp-down phase, was conducted to determine the yield stress and plastic viscosity of the selected pastes. The pre-shear phase consisted of ramping up from an initial shear rate of 10/s to 100/s in 75 s to homogenize the paste, followed immediately by a ramp-down to 0.005/s. This phase is followed by a ramp-up phase from 0.005/s to 100/s and a ramp-down phase from 100/s to 0.005/s. This procedure is represented graphically in Figure 2. Excluding the pre-shear phase, data are acquired every second until three consecutive torque measurements are within  $<8\%$  of each other. At this time, the experiment advances to the next shear rate. The yield stress and plastic viscosity of the activated pastes are determined by using the Bingham model. The Bingham model fits a linear model to the flow curves (shear stress vs. shear rate) as per Equation (1).

$$\tau = \mu_p \gamma + \tau_y \tag{1}$$

where  $\tau$  = shear stress (Pa);  $\mu_p$  = plastic viscosity (Pa-s);  $\gamma$  = shear rate (1/s); and  $\tau_y$  = yield stress (Pa).

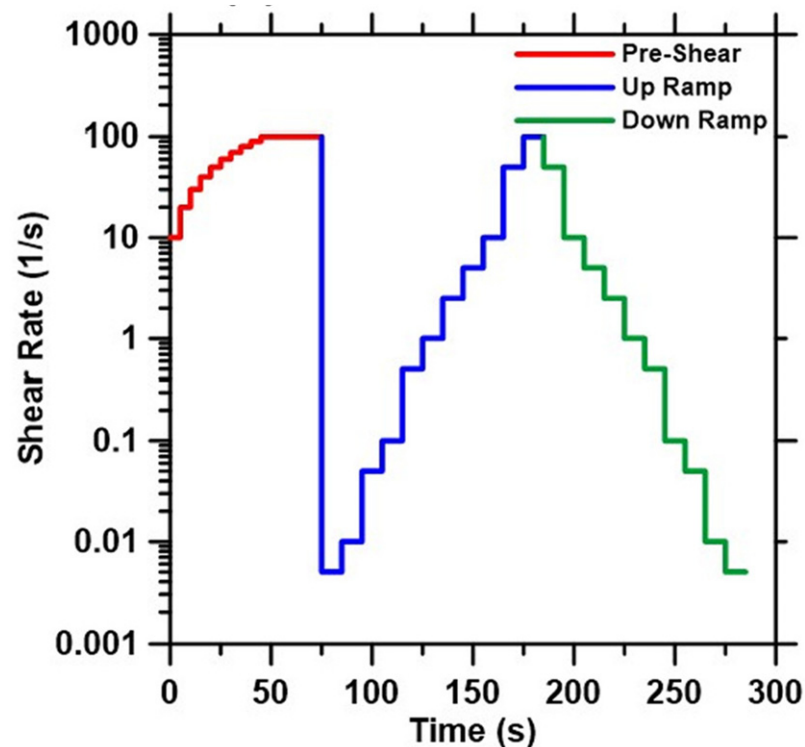


Figure 2. Representation of the strain-controlled rheological procedure.

### 3. Results and Discussion

#### 3.1. Setting Times

Setting time is used here to identify acceptable binder compositions and activator parameters ( $n$  and  $M_s$  values) for further studies on rheology, reaction kinetics, and mechanical properties. When using solid activators, in this case, solid K–Si, alkali-activated binders can be prepared either by blending the solid activator with the binder constituents and then adding the requisite amount of mixing water or adding a premixed activator solution made from the solid activator (cooled to room temperature) directly, in which case the desired amounts of solid activator and corresponding hydroxide are dissolved in water at room temperature. It is essential to note that the preparation method could influence the early-age properties of the binder. In this study, the solid K–Si and KOH were dissolved in water at room temperature and allowed to cool down before mixing the solution with the binder ingredients. However, it is also possible to add the solid activator directly to the powder so as to create one-part alkali-activated binder systems, as demonstrated in our previous work [41].

The initial and final setting times of all the binder mixtures examined here are shown in Table 3. The setting times are generally found to decrease with an increase in slag content in the binder system. This is attributable to the enhanced availability of  $\text{Ca}^{2+}$  ions (liberated from the surface of the slag particles) that combine with  $[\text{SiO}_4]^{4-}$  ions liberated from Na–Si or K–Si, enhancing the amount of early reaction product formation [44,45]. The  $\text{Na}_2\text{O}$  content (proportional to the  $n$  value) has a significant effect on the setting times, as has been elucidated in our previous work on pure fly ash or slag-based activated binders [38]. In this study, it is observed that the set times are delayed with an increase in the  $n$  value of the activator solutions, indicating that there is an ideal pH range that influences setting times, as noted elsewhere, as well [46]. A high pH level increases the presence of Si and Al in the solution while decreasing the concentration of Ca. A higher silicate concentration in the activator also hinders the precipitation kinetics of aluminates phases in slag [44,46], leading to reduced set times.

**Table 3.** Initial and final setting times of MT-S blends comprising 20% and 30% slag content by mass and prepared with liquid sodium (Na)-silicate (Si), liquid potassium (K)-silicate (Si), and solid potassium (K)-silicate (Si) at different  $n$  and  $M_s$  values used in this study.

Binder Composition	Activator Parameters			Initial Setting Time (min)	Final Setting Time (min)	
	Activator Type	$M_s$	$n$			
80 Mine tailing (MT)-20 slag (S)	Liquid sodium (Na)-silicate (Si)	1.0	0.050	92	108	
			0.075	94	200	
		1.5	0.050	58	93	
			0.075	124	177	
		70 Mine tailing (MT)-30 slag (S)	1.0	0.050	39	90
				0.075	58	101
80 Mine tailing (MT)-20 slag (S)	Liquid potassium (K)-silicate (Si)	1.5	0.050	42	63	
			0.075	74	106	
		1.0	0.050	15	48	
			0.075	23	38	
		70 Mine tailing (MT)-30 slag (S)	1.5	0.050	297	573
				0.075	>720	- *
80 Mine tailing (MT)-20 slag (S)	Solid potassium (K)-silicate (Si)	1.0	0.050	14	37	
			0.075	15	27	
		70 Mine tailing (MT)-30 slag (S)	1.5	0.050	146	196
				0.075	287.75	766
		80 Mine tailing (MT)-20 slag (S)	1.0	0.050	26	61
				0.075	27	47
70 Mine tailing (MT)-30 slag (S)	Solid potassium (K)-silicate (Si)	1.5	0.050	718	825	
			0.075	>720	-	
		1.0	0.050	16	29	
			0.075	21	39	
		80 Mine tailing (MT)-20 slag (S)	1.5	0.050	222	245
				0.075	668	726

\*—Final setting time for blends with initial setting time > 720 min was not recorded.

The setting times are more susceptible to changes in  $M_s$  values than  $n$  values, further emphasizing the influence of silicate species from the activator on the very early reaction mechanisms. Setting times for all the MT-S blends prepared in this study increase considerably with an increase in  $M_s$  value, which is attributed to the excess silicates and not enough alkaline species to sever the silica ions in silicate chains and incorporate the aluminum ion in the gel structure to form calcium aluminosilicate hydrate (C-(A)-S-H) gel in the presence of  $M^+$  ions [40,47,48]. At a lower  $M_s$  value, the higher alkalinity of the systems enhances the initial dissolution rate for both Na-Si- and K-Si-activated blends, with consequent precipitation of an insoluble, low Ca/Si molar ratio product (Al-rich gel). There is a higher amount of  $OH^-$  ions in the solution to break further Si-O and Al-O bonds to react with  $Ca^{2+}$  ions to form C-(A)-S-H gel, in these cases. The solid K-Si-activated MT-S blends have higher setting times than their counterparts activated using liquid K-Si, which is attributable to the reduced levels of silica dissolution from solid activators [38], which impedes the formation of hydration reaction products. The MT-S blends with faster initial setting times can be used in repair applications.

### 3.2. Rheological Characterization

Figure 3 shows the yield stress and plastic viscosity of the activated MT-S binders used in this study. The yield stress is defined as the minimum stress required to initiate or maintain flow, and the resistance offered by a fluid to flow freely is quantified as plastic viscosity. The rheological characteristics of suspensions typically depend on the volume and characteristics of the suspending fluid and the size, shape, and concentration of the suspending particles [49–52]. The variation in rheological parameters of MT-S binders as a function of slag content and activator type and parameters are shown in Figure 3. Na-Si-activated MT-S binders demonstrate significantly lower yield stress and plastic viscosity than the K-Si-activated binders proportioned using similar  $n$  and  $M_s$  values. This can be explained by considering the difference in the rheological behavior of the NaOH and KOH solutions and the silicate-bearing activators. The presence of colloidal Si-O-H-M complexes (where M denotes Na or K species) in concentrated alkali solutions increases the solution viscosity [53]. At equivalent concentrations, the viscosity of the NaOH solution is significantly higher than the corresponding KOH solution (for example, ~3 times higher at a concentration of 8 mol/L), which is attributable to the higher charge density of  $\text{Na}^+$  ions resulting in higher ion-dipole forces in the NaOH solutions. Note that to obtain identical  $n$  and  $M_s$  values for N-Si and K-Si activators, more Na-Si is needed (than K-Si) due to the lower molecular weight of sodium. This results in non-equivalent ion-dipole forces in these solutions, resulting in Na-bearing silicate solutions showing higher viscosities. Thus, the overall higher viscosity of the activator solution comprising Na-Si and NaOH compared to the solution containing K-Si and KOH is responsible for the higher viscosity and yield stress of the Na-Si-activated MT-S binders.

The yield stress of MT-S binders activated using the same activator decreases with increasing slag content at similar  $n$  and  $M_s$  values. Yield stress reduction has also been noticed with increasing the slag addition in Portland cement pastes [54], and the behavior is attributed to the changes in resultant interparticle forces (van der Waals forces). As the slag content in the binder increases, the homogeneity of the mixture decreases, and the interparticle spacing between the MT particles increases, consequentially reducing the interparticle attraction forces between them, resulting in the reduction in the yield stress of the pastes. Similar observations are reported in another study, where adding limestone to the cement binder reduced yield stress [55]. The yield stress of Na-Si-activated binders increases with an increase in  $n$  or  $M_s$  value at a similar slag content. This is primarily attributed to increased activator solution viscosity, as explained earlier.

For K-Si-activated binders, the yield stress approaches zero, suggesting Newtonian behavior, an observation that has been reported on alkali-activated fly ash suspensions [56]. Increasing the  $n$  value decreases the yield stress of the K-Si-activated binders, while the plastic viscosities are rather invariant. Increasing the amount of activator solution increases the particle spacing, thereby increasing the fluid film thickness around the binder particles, thus decreasing the yield stress [56]. The effect is prominent in K-Si-activated binders likely due to the lower viscosity of the K-Si activator solution, as mentioned earlier. Both the activation solution viscosity and the alkali cation are found to greatly influence the rheology of activated MT-S binders, and thus demand careful attention during mixture design and optimization.

### 3.3. Isothermal Calorimetry

Figure 4a,b shows the heat evolution curves up to 48 h for liquid Na-Si-activated MT-S blends proportioned using  $n$  values of 0.05 and 0.075 and  $M_s$  values of 1.0 and 1.5. The heat evolution curves for liquid K-Si-activated MT-S blends are presented in Figure 4c,d, while for those activated using solid K-Si, the curves are shown in Figure 4e,f. Table 4 comprehensively summarizes the salient observations obtained from the isothermal calorimetry tests for all the blends and activator parameters used in this study.

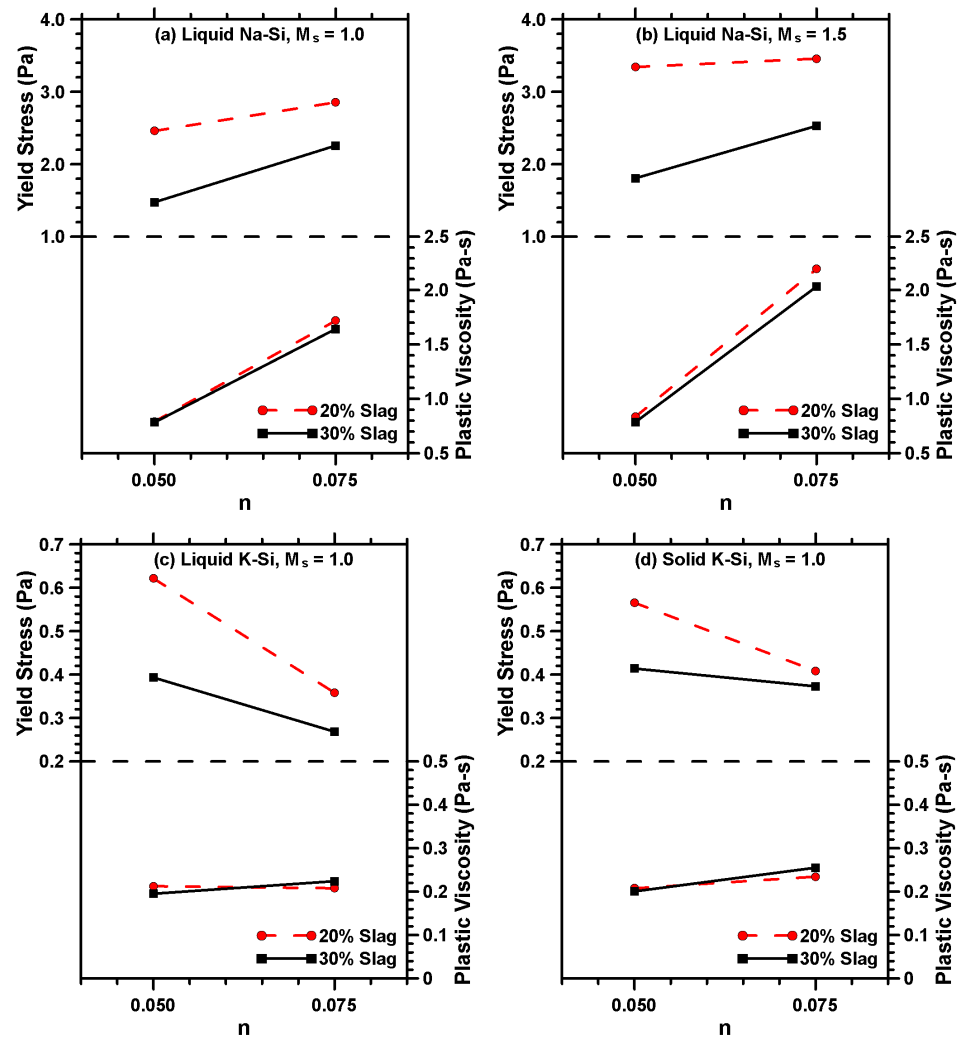


**Figure 3.** Rheological properties of liquid sodium (Na)–silicate (Si)-activated MT–S blends prepared with  $M_s$  values of (a) 1.0 and (b) 1.5; (c) liquid potassium (K)–silicate (Si)-activated MT–S blends prepared with an  $M_s$  value of 1.0, and; (d) solid potassium (K)–silicate (Si)-activated MT–S blends prepared with an  $M_s$  value of 1.0.

An increase in slag content increases the cumulative heat released, irrespective of the activator type, attributable to an increase in the amount of  $Ca^{2+}$  ions that combine with  $[SiO_4]^{4-}$  ions liberated from the activator solution, enhancing the hydration product formation [44]. The increase is more pronounced at higher alkalinity levels, attained using a lower  $M_s$  value combined with a higher  $n$  value. This is expected, since higher alkalinity results in an increased dissolution of silica along with the liberation of  $Ca^{2+}$  ions, and thus increases the potential for the formation of more amounts of reaction products, such as C–(A)–S–H gel. The alkali activation parameters also significantly influence the heat release behavior. When the  $M_s$  value is lowered through the addition of alkali hydroxides, the initial dissolution rate is enhanced for both Na–Si- and K–Si-activated mixtures [40], which is evident from the higher initial heat release peak for all the activated MT–S blends proportioned using a  $M_s$  value of 1.0 compared to those prepared using a  $M_s$  value of 1.5, as noticed in Figure 4. The effect is more pronounced at a higher slag content and alkalinity (attained by using a higher  $n$  value). The magnitude of the first peak heat release and the increases with the increase in  $n$  value are attributable to improved reaction kinetics due to the higher alkalinity of the system, as explained earlier. The cumulative heat released for K–Si-activated MT–S blends (see Table 4) proportioned using an  $M_s$  value of 1.5 is relatively insignificant, indicating that the alkalinity levels produced are not sufficient,

even though the initial heat release peak is higher compared to the Na–Si-activated MT–S blends at similar  $n$  values and an  $M_s$  of 1.5. This brings out the cationic influence on activation reactions, especially in conjunction with the concentration in the anionic (e.g., silicate) species, as evidenced by the low cumulative heat release (and negligible strengths) at higher  $M_s$  values when K–Si is used as an activator.

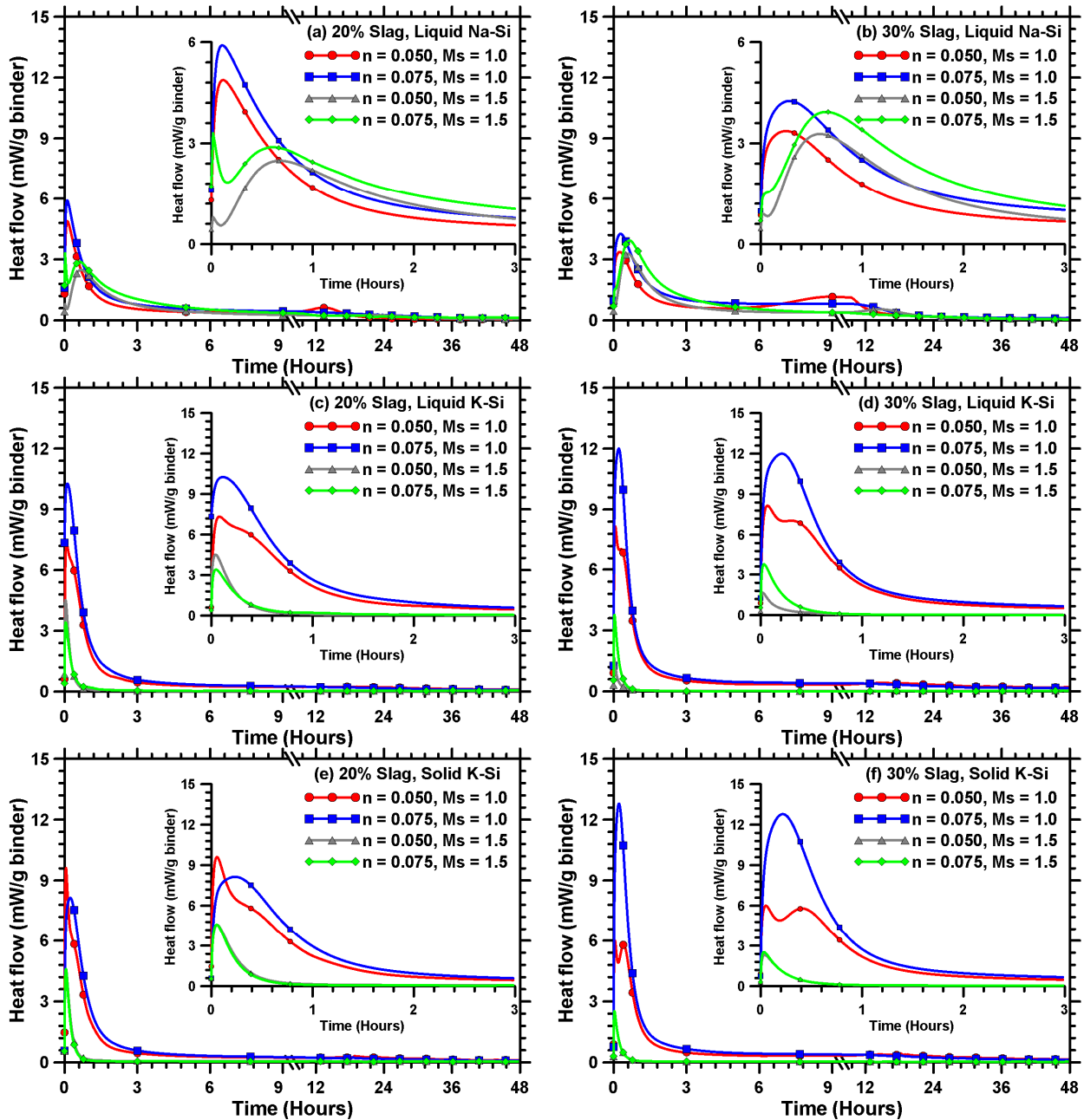


**Figure 4.** Heat release rate curves for liquid sodium (Na)–silicate (Si)-activated MT–S blends with slag contents of (a) 20% and (b) 30%; liquid potassium (K)–silicate (Si)-activated MT–S blends with slag contents of (c) 20% and (d) 30%; and solid potassium (K)–silicate (Si)-activated MT–S blends with slag contents of (e) 20% and (f) 30%.

**Table 4.** Heat release response parameters of MT–S blends comprising 20% and 30% slag content by mass and prepared with liquid sodium (Na)–silicate (Si), liquid potassium (K)–silicate (Si), and solid potassium (K)–silicate (Si) at different  $n$  and  $M_s$  values used in this study.

Binder Composition	Activation Parameters			Magnitude of Peak (mW/g Binder)		Time to Peak (h)		Cumulative Heat (J/g Binder)		
	Activator Type	$M_s$	$n$	First Peak	Second Peak	First Peak	Second Peak			
80 Mine tailing (MT)–20 slag (S)	Liquid sodium (Na)–silicate (Si)	1.00	0.050	4.88	0.63	0.12	13.40	53.41		
			0.075	5.90	-	0.12	-	65.89		
		1.50	0.050	0.81	2.49	0.02	0.70	48.32		
			0.075	3.30	2.89	0.02	0.60	58.97		
		70 Mine tailing (MT)–30 slag (S)	Liquid sodium (Na)–silicate (Si)	1.00	0.050	3.37	1.17	0.25	9.00	67.61
					0.075	4.26	-	0.28	-	78.81
1.50	0.050			0.91	3.28	0.02	0.58	57.84		
	0.075			3.94	-	0.65	-	61.65		
80 Mine tailing (MT)–20 slag (S)	Liquid potassium (K)–silicate (Si)	1.00	0.050	7.34	-	0.08	-	55.28		
			0.075	10.27	-	0.12	-	61.18		
		1.50	0.050	4.52	-	0.04	-	9.46		
			0.075	3.41	-	0.05	-	11.60		
		70 Mine tailing (MT)–30 slag (S)	Liquid potassium (K)–silicate (Si)	1.00	0.050	8.16	-	0.07	-	75.80
					0.075	12.00	-	0.21	-	80.19
1.50	0.050			1.65	-	0.02	-	6.25		
	0.075			3.76	-	0.03	-	6.41		
80 Mine tailing (MT)–20 slag (S)	Powdered potassium (K)–silicate (Si)	1.00	0.050	9.61	-	0.05	-	58.34		
			0.075	8.15	-	0.23	-	59.72		
		1.50	0.050	4.59	-	0.06	-	15.14		
			0.075	4.59	-	0.05	-	12.47		
		70 Mine tailing (MT)–30 slag (S)	Powdered potassium (K)–silicate (Si)	1.00	0.050	6.01	5.80	0.05	0.40	68.27
					0.075	12.79	-	0.22	-	78.89
1.50	0.050			2.32	-	0.04	-	8.36		
	0.075			2.52	-	0.03	-	8.95		

The calorimetric response for liquid Na–Si-activated MT–S blends (Figure 4a,b) prepared at higher alkalinity levels (higher  $n$  value and lower  $M_s$  value) shows a single major heat release peak, which is attributed to the combination of both the wetting and dissolution of binder particles and the formation of early reaction products [37]. It has also been reported that at higher alkalinity levels, the larger early peak could mask the subsequent peak and, in some cases, may just be detected as a shoulder in the main peak [44]. At lower alkalinity, a second heat release peak is observed shortly after the first heat release peak. The second heat release peak is observed at much later times for MT–S blends proportioned using an  $n$  value of 0.05 and  $M_s$  of 1.0. Here, the first narrow peak within the first few hours of mixing corresponds to the wetting and dissolution of the Ca-bearing compounds [38,45]. The initial peak is followed by a dormant period, which is succeeded by an acceleration peak that is smaller in magnitude and is generally attributed to the formation of reaction products, such as calcium silicate hydrate (C–S–H) and C–(A)–S–H gels [57]. The K–Si-activated MT–S blends show a significantly higher heat release peak than their Na–Si-activated counterparts, as shown in Figure 4c–f (though the total heat released after 48 h is negligible at higher  $M_s$  values, as shown in Table 4). For instance, the magnitude of single peak heat release for the MT–S blend comprising 30% slag content and proportioned at an  $n$  and  $M_s$  value of 0.075 and 1.0 increases from 4.23 mW/g binder to 12.0 mW/g binder, and 12.79 mW/g binder when activated with liquid K–Si and solid K–Si, respectively, instead of liquid Na–Si. This is in line with our previous study, where K-silicate-activated slag pastes demonstrated higher intensities of acceleration peak and higher rates of the reaction acceleration phase [40]. The smaller ionic radius of the solvated

K<sup>+</sup> ion [58,59] results in faster ionic movement through the system and, thus, a reduced dormant period and a more intense acceleration peak [40]. Furthermore, the lower viscosity of the K–Si activator solution than the Na–Si activator solution also contributes to faster ionic movement and consequently increased reactivity and heat release [56].

### 3.4. Compressive Strength

The compressive strengths of Na–Si- and K–Si-activated MT–S mortar binders were determined after 3, 7, 14, and 28 days of moist curing to understand the influence of curing age, slag content, activator parameters, and cationic species on the mechanical properties of the binder. Figure 5a,b shows the strength development of liquid Na–Si-activated MT–S binders comprising 20% and 30% slag content by mass of binder, respectively. The compressive strength development of the liquid and solid K–Si-activated MT–S binders is shown in Figure 5c,d. The MT–S binders activated using a liquid or solid K–Si activator having an  $M_s$  value of 1.5 showed strengths  $\leq 2$  MPa, even after 28 days of curing; thus, they are not shown here. This is in line with isothermal calorimetry results, where the cumulative heat released at the end of 48 h was significantly lower ( $\leq 16$  J/g binder) for liquid or solid K–Si-activated MT–S blends at this  $M_s$  value compared to all other blends ( $\geq 48$  J/g binder), as explained earlier.

The rate of strength development shown in Figure 5 provides an indication of the time-dependent formation of reaction products and consequent space filling. It can be seen from Figure 5 that the compressive strengths of all the MT–S mortars increase with an increase in  $n$  value. This can be attributed to the following reasons: (i) the increased amount of OH<sup>−</sup> ions in the solution results in an increased dissolution of the Si along with the liberation of Ca<sup>2+</sup>, increasing the potential for the formation of C–(A)–s–H gels [60]; (ii) the water-impermeable layer on the surface of the binder particles is disturbed by the alkaline activator, leading to faster reaction rates and formation of more reaction products [61,62]; and (iii) more sodium silicate is present in the activator solution at a higher  $n$  value, resulting in the formation of more silica-containing gel (due to a higher concentration of [SiO<sub>4</sub>]<sup>4−</sup> ions), lowering the Ca/Si ratio of the reaction products, which is also reported to result in higher compressive strengths [42]. Similar reasons can be used to explain the increase in compressive strengths of liquid Na–Si-activated MT–S binders when a lower  $M_s$  value is used. The increase in strength observed between the 3rd and 28th days is relatively minimal when the alkalinity levels are low ( $n$  value of 0.05). However, at higher alkalinity levels ( $n$  value of 0.075), a noticeable improvement in strength is evident from the 14th to 28th days, as observed in Figure 5.

An increase in slag content increases the compressive strengths of MT–S binders, irrespective of the activator type and parameters. This is attributable to the formation of more amounts of strength-imparting reaction products, such as C–(A)–s–H gel. The compressive strengths for MT–S binders proportioned at an  $n$  value of 0.05 and  $M_s$  of 1.0, and activated using liquid Na–Si, liquid K–Si, and solid K–Si, increased from 14.5 MPa, 11.7 MPa, and 12.07 MPa, to 29.3 MPa, 17.5 MPa, and 20.8 MPa, respectively, when the slag content in the binder increased from 20% to 30%. In general, the compressive strengths of liquid Na–Si-activated binders were higher than those activated using liquid or solid K–Si activators, attributable to the increased amounts of reaction product formation in Na–Si-activated systems [40] and the likely enhancement in the degree of silicate polymerization, since the Na<sup>+</sup> cation better coagulates with monomeric silicates species [63]. The compressive strengths of solid K–Si-activated mortars are found to be marginally higher than mortars activated using liquid K–Si.

Overall, alkali activation of MT–S binders allows the production of sustainable binders containing MT as their primary constituent, with 28-day compressive strengths ranging from 10–35 MPa, which is appropriate for many concrete applications. MT–S concretes with even higher strengths can be produced by increasing the slag content (e.g., up to 50%). Even though higher alkalinity has been shown to lead to further strength enhancements, it is preferred to maintain the alkali content below a certain threshold, since higher amounts

could contribute to carbonation and leaching [34,64]. It is thus important to optimize the mix proportions (binder ingredients and activator parameters) to ensure the desired performance of MT-based binders.

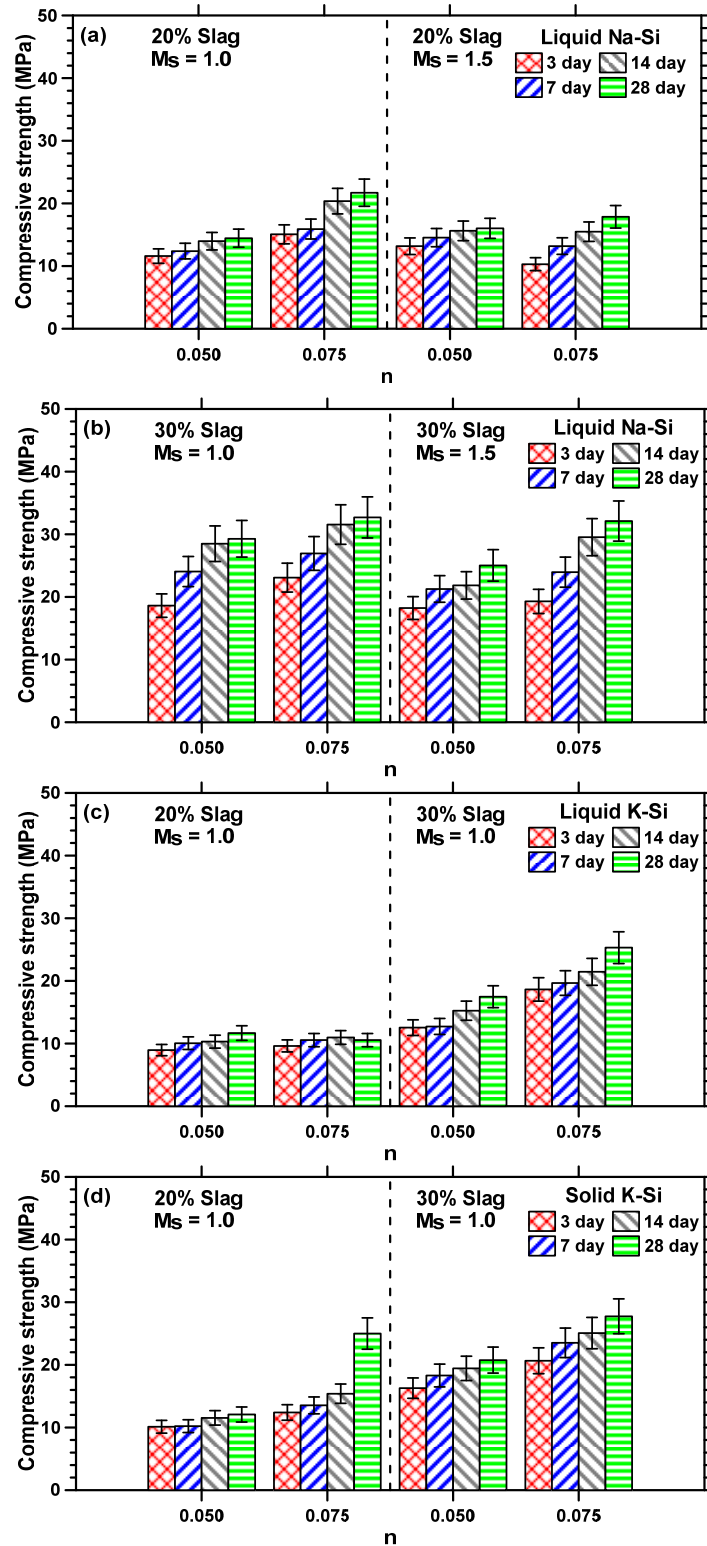


**Figure 5.** Compressive strength development of liquid sodium (Na)-silicate (Si)-activated MT-S blends with slag contents of (a) 20% and (b) 30%; (c) liquid potassium (K)-silicate (Si)-activated MT-S blends prepared at an  $M_s$  value of 1.0; (d) solid potassium (K)-silicate (Si)-activated MT-S blends prepared at an  $M_s$  value of 1.0.

#### 4. Conclusions

The study explored the impact of varying levels of alkalinity, represented by the  $M_2O$ -to-binder ratio ( $n$ ) ( $M$  being the  $Na^+$  or  $K^+$  cation), as well as the activator's  $SiO_2$ -to- $M_2O$  ratio ( $M_s$ ) on setting times, rheological characteristics (yield stress and plastic viscosity, specifically), early-stage hydration kinetics, and compressive strength development of mine tailing (MT)-based binder systems. Three distinct activators were used: liquid sodium (Na)-silicate (Si), liquid potassium (K)-silicate (Si), and solid potassium (K)-silicate (Si), in combination with NaOH or KOH to reduce the silica modulus as desired. Slag was used as a minor additive (20% and 30% by mass of MT); higher levels of slag expedited early reaction product formation. The significance of the  $M_s$  value on setting times was revealed; elevated  $M_s$  values corresponded to prolonged setting times. Liquid K-Si-activated blends exhibited shorter setting times compared to the liquid Na-Si-activated blends due to higher early-age reactivity, facilitated by the higher ionic mobility of solvated  $K^+$  ions. However, blends activated by solid K-Si demonstrated extended setting times compared to their liquid K-Si counterparts due to limited silica dissolution from solid activators. The effects of the physical state of the activator on early-age reaction mechanisms were thus identified.

Yield stress was found to decrease as the slag content increased. Na-Si-activated binders displayed an increase in yield stress, with higher  $n$  or  $M_s$  values, because of the higher activator solution viscosity. On the other hand, K-Si-activated binders manifested a Newtonian behavior. Elevating the  $n$  value in K-Si binders diminished yield stress, while plastic viscosities remained relatively stable. Isothermal calorimetry tests showed that liquid K-Si-activated blends display higher heat release peaks than liquid Na-Si-activated blends, indicative of greater early-age reactivity. In addition, improved alkalinity achieved through lowered  $M_s$  or elevated  $n$  positively affected heat release for both Na-Si- and K-Si-activated blends. Examinations of compressive strength revealed that Na-Si-activated binders outperformed their K-Si-activated counterparts, primarily due to increased reaction product formation and enhanced silicate polymerization. Elevating slag content in the binder formulations enhanced the compressive strengths, as expected.

This work has highlighted the pivotal role of activation parameters and binder constituents in determining the attributes of alkali-activated MT-S binders. A comprehensive understanding of these parameters' effects on setting time, rheology parameters, reactivity, and mechanical properties is essential in the selection of optimal mixture parameters, which can be tailored to attain specific properties for the intended applications, as well as to maximize the content of waste or by-product materials in these applications, which eventually will reduce the  $CO_2$  impact of binder systems. While it is also critical to evaluate the durability properties, such as ionic and moisture transport characteristics, leaching behavior, etc., of these materials to ensure their suitable field implementation, this is not described in this paper.

**Author Contributions:** Conceptualization, N.N. and S.S.; methodology, S.S. and R.K.R.; validation, S.S. and A.S.; formal analysis, S.S.; investigation, S.S., R.K.R. and A.S.; resources, N.N.; data curation, S.S., R.K.R. and A.S.; writing—original draft preparation, S.S.; writing—review and editing, N.N.; supervision, N.N.; project administration, N.N.; funding acquisition, N.N. All authors have read and agreed to the published version of the manuscript.

**Funding:** The authors sincerely acknowledge Freeport McMoRan Inc. for supplying the mine tailings and for financial support of this work through the NSF Engineering Research Center on Bio-Mediated and Bio-Inspired Geotechnics (CBBG) at ASU (EEC 1449501). The NSF Future Manufacturing grant (DMR 2228782) is also acknowledged.

**Data Availability Statement:** The raw/processed data required to reproduce these findings cannot be shared at this time as the data also forms part of an ongoing study.

**Acknowledgments:** The authors sincerely acknowledge Freeport McMoRan Inc. for supplying the mine tailings and for financial support of this work through the NSF Engineering Research Center on Bio-Mediated and Bio-Inspired Geotechnics (CBBG) at ASU. The slag used in this work was supplied

by Cemex, and PQ Corp supplied the sodium silicate and potassium silicate. Their contributions are also acknowledged.

**Conflicts of Interest:** The raw/processed data required to reproduce these findings cannot be shared at this time as the data also forms part of an ongoing study.

## References

1. Maruthupandian, S.; Chaliasou, A.; Kanellopoulos, A. Recycling mine tailings as precursors for cementitious binders—Methods, challenges and future outlook. *Constr. Build. Mater.* **2021**, *312*, 125333. [[CrossRef](#)]
2. Qaidi, S.M.A.; Tayeh, B.A.; Zeyad, A.M.; de Azevedo, A.R.G.; Ahmed, H.U.; Emad, W. Recycling of mine tailings for the geopolymers production: A systematic review. *Case Stud. Constr. Mater.* **2022**, *16*, e00933. [[CrossRef](#)]
3. Krishna, R.S.; Shaikh, F.; Mishra, J.; Lazorenko, G.; Kasprzhitskii, A. Mine tailings-based geopolymers: Properties, applications and industrial prospects. *Ceram. Int.* **2021**, *47*, 17826–17843. [[CrossRef](#)]
4. Ince, C.; Derogar, S.; Gurbakay, K.; Ball, R.J. Properties, durability and cost efficiency of cement and hydrated lime mortars reusing copper mine tailings of Lefke-Xeros in Cyprus. *Constr. Build. Mater.* **2021**, *268*, 121070. [[CrossRef](#)]
5. Vilela, A.P.; Eugênio, T.M.C.; de Oliveira, F.F.; Mendes, J.F.; Ribeiro, A.G.C.; Brandão, L.E.V.D.S.; Mendes, R.F. Technological properties of soil-cement bricks produced with iron ore mining waste. *Constr. Build. Mater.* **2020**, *262*, 120883. [[CrossRef](#)]
6. Dong, L.; Tong, X.; Li, X.; Zhou, J.; Wang, S.; Liu, B. Some developments and new insights of environmental problems and deep mining strategy for cleaner production in mines. *J. Clean. Prod.* **2019**, *210*, 1562–1578. [[CrossRef](#)]
7. Nurcholis, M.; Yudiantoro, D.F.; Haryanto, D.; Mirzam, A. Heavy Metals Distribution in the Artisanal Gold Mining Area in Wonogiri. *Indones. J. Geogr.* **2017**, *49*, 133–144. [[CrossRef](#)]
8. Macklin, M.G.; Brewer, P.A.; Balteanu, D.; Coulthard, T.J.; Driga, B.; Howard, A.J.; Zaharia, S. The long term fate and environmental significance of contaminant metals released by the January and March 2000 mining tailings dam failures in Maramureş County, upper Tisa Basin, Romania. *Appl. Geochem.* **2003**, *18*, 241–257. [[CrossRef](#)]
9. Macklin, M.; Brewer, P.; Hudson-Edwards, K.; Bird, G.; Coulthard, T.; Dennis, I.; Lechler, P.; Miller, J.; Turner, J. A geomorphological approach to the management of rivers contaminated by metal mining. *Geomorphology* **2006**, *79*, 423–447. [[CrossRef](#)]
10. Rico, M.; Benito, G.; Díez-Herrero, A. Floods from tailings dam failures. *J. Hazard. Mater.* **2008**, *154*, 79–87. [[CrossRef](#)]
11. Liu, H.; Probst, A.; Liao, B. Metal contamination of soils and crops affected by the Chenzhou lead/zinc mine spill (Hunan, China). *Sci. Total Environ.* **2005**, *339*, 153–166. [[CrossRef](#)] [[PubMed](#)]
12. Rzymiski, P.; Klimasyk, P.; Marszelewski, W.; Borowiak, D.; Mleczek, M.; Nowiński, K.; Pius, B.; Niedzielski, P.; Poniedziałek, B. The chemistry and toxicity of discharge waters from copper mine tailing impoundment in the valley of the Apuseni Mountains in Romania. *Environ. Sci. Pollut. Res. Int.* **2017**, *24*, 21445–21458. [[CrossRef](#)] [[PubMed](#)]
13. Provis, J.L. Alkali-activated materials. *Cem. Concr. Res.* **2018**, *114*, 40–48. [[CrossRef](#)]
14. Akinyemi, B.A.; Alaba, P.A.; Rashedi, A. Selected performance of alkali-activated mine tailings as cementitious composites: A review. *J. Build. Eng.* **2022**, *50*, 104154. [[CrossRef](#)]
15. Araujo, F.S.M.; Taborda-Llano, I.; Nunes, E.B.; Santos, R.M. Recycling and Reuse of Mine Tailings: A Review of Advancements and Their Implications. *Geosciences* **2022**, *12*, 319. [[CrossRef](#)]
16. Guo, J.; Bao, Y.; Wang, M. Steel slag in China: Treatment, recycling, and management. *Waste Manag.* **2018**, *78*, 318–330. [[CrossRef](#)] [[PubMed](#)]
17. Rao, F.; Liu, Q. Geopolymerization and Its Potential Application in Mine Tailings Consolidation: A Review. *Miner. Process. Extr. Metall. Rev.* **2015**, *36*, 399–409. [[CrossRef](#)]
18. Alonso, M.; Pasko, A.; Gascó, C.; Suarez, J.; Kovalchuk, O.; Krivenko, P.; Puertas, F. Radioactivity and Pb and Ni immobilization in SCM-bearing alkali-activated matrices. *Constr. Build. Mater.* **2018**, *159*, 745–754. [[CrossRef](#)]
19. Ercikdi, B.; Cihangir, F.; Kesimal, A.; Deveci, H. Practical Importance of Tailings for Cemented Paste Backfill. In *Paste Tailings Management*; Yilmaz, E., Fall, M., Eds.; Springer International Publishing: Cham, Switzerland, 2017; pp. 7–32. [[CrossRef](#)]
20. Lazorenko, G.; Kasprzhitskii, A.; Shaikh, F.; Krishna, R.S.; Mishra, J. Utilization potential of mine tailings in geopolymers: Physicochemical and environmental aspects. *Process Saf. Environ. Prot.* **2021**, *147*, 559–577. [[CrossRef](#)]
21. He, X.; Yuhua, Z.; Qaidi, S.; Isleem, H.F.; Zaid, O.; Althoey, F.; Ahmad, J. Mine tailings-based geopolymers: A comprehensive review. *Ceram. Int.* **2022**, *48*, 24192–24212. [[CrossRef](#)]
22. Zhao, S.; Xia, M.; Yu, L.; Huang, X.; Jiao, B.; Li, D. Optimization for the preparation of composite geopolymer using response surface methodology and its application in lead-zinc tailings solidification. *Constr. Build. Mater.* **2021**, *266*, 120969. [[CrossRef](#)]
23. Zhang, N.; Hedayat, A.; Sosa, H.G.B.; Cárdenas, J.J.G.; Álvarez, G.E.S.; Rivera, V.B.A. Specimen size effects on the mechanical behaviors and failure patterns of the mine tailings-based geopolymer under uniaxial compression. *Constr. Build. Mater.* **2021**, *281*, 122525. [[CrossRef](#)]
24. Ghazi, A.B.; Jamshidi-Zanjani, A.; Nejati, H. Utilization of copper mine tailings as a partial substitute for cement in concrete construction. *Constr. Build. Mater.* **2022**, *317*, 125921. [[CrossRef](#)]
25. Xiaolong, Z.; Shiyu, Z.; Hui, L.; Yingliang, Z. Disposal of mine tailings via geopolymerization. *J. Clean. Prod.* **2021**, *284*, 124756. [[CrossRef](#)]

26. Lyu, X.; Yao, G.; Wang, Z.; Wang, Q.; Li, L. Hydration kinetics and properties of cement blended with mechanically activated gold mine tailings. *Thermochim. Acta* **2020**, *683*, 178457. [[CrossRef](#)]
27. Zhang, X.; Han, Y.; Gao, P.; Li, Y. Effects of grinding media on grinding products and flotation performance of chalcopyrite. *Miner. Eng.* **2020**, *145*, 106070. [[CrossRef](#)]
28. Khalifa, A.Z.; Cizer, Ö.; Pontikes, Y.; Heath, A.; Patureau, P.; Bernal, S.A.; Marsh, A.T. Advances in alkali-activation of clay minerals. *Cem. Concr. Res.* **2020**, *132*, 106050. [[CrossRef](#)]
29. Zhang, Z.; Wang, H.; Yao, X.; Zhu, Y. Effects of halloysite in kaolin on the formation and properties of geopolymers. *Cem. Concr. Compos.* **2012**, *34*, 709–715. [[CrossRef](#)]
30. Chelgani, S.C.; Parian, M.; Parapari, P.S.; Ghorbani, Y.; Rosenkranz, J. A comparative study on the effects of dry and wet grinding on mineral flotation separation—a review. *J. Mater. Res. Technol.* **2019**, *8*, 5004–5011. [[CrossRef](#)]
31. Bernal, S.A.; Provis, J.L. Durability of Alkali-Activated Materials: Progress and Perspectives. *J. Am. Ceram. Soc.* **2014**, *97*, 997–1008. [[CrossRef](#)]
32. Pacheco-Torgal, F.; Castro-Gomes, J.; Jalali, S. Alkali-activated binders: A review: Part 1. Historical background, terminology, reaction mechanisms and hydration products. *Constr. Build. Mater.* **2008**, *22*, 1305–1314. [[CrossRef](#)]
33. Duxson, P.; Fernández-Jiménez, A.; Provis, J.L.; Lukey, G.C.; Palomo, A.; van Deventer, J.S.J. Geopolymer technology: The current state of the art. *J. Mater. Sci.* **2007**, *42*, 2917–2933. [[CrossRef](#)]
34. Wang, S.-D.; Scrivener, K.L. Hydration products of alkali activated slag cement. *Cem. Concr. Res.* **1995**, *25*, 561–571. [[CrossRef](#)]
35. Fernández-Jiménez, A.; Palomo, J.G.; Puertas, F. Alkali-activated slag mortars: Mechanical strength behaviour. *Cem. Concr. Res.* **1999**, *29*, 1313–1321. [[CrossRef](#)]
36. Zhang, Z.; Provis, J.L.; Zou, J.; Reid, A.; Wang, H. Toward an indexing approach to evaluate fly ashes for geopolymer manufacture. *Cem. Concr. Res.* **2016**, *85*, 163–173. [[CrossRef](#)]
37. Ravikumar, D.; Neithalath, N. Reaction kinetics in sodium silicate powder and liquid activated slag binders evaluated using isothermal calorimetry. *Thermochim. Acta* **2012**, *546*, 32–43. [[CrossRef](#)]
38. Chithiraputhiran, S.; Neithalath, N. Isothermal reaction kinetics and temperature dependence of alkali activation of slag, fly ash and their blends. *Constr. Build. Mater.* **2013**, *45*, 233–242. [[CrossRef](#)]
39. Zhang, Z.; Provis, J.L.; Reid, A.; Wang, H. Fly ash-based geopolymers: The relationship between composition, pore structure and efflorescence. *Cem. Concr. Res.* **2014**, *64*, 30–41. [[CrossRef](#)]
40. Dakhane, A.; Peng, Z.; Marzke, R.; Neithalath, N. Comparative Analysis of the Influence of Sodium and Potassium Silicate Solutions on the Kinetics and Products of Slag Activation. *Adv. Civ. Eng. Matls.* **2014**, *3*, 371–387. [[CrossRef](#)]
41. Dakhane, A.; Neithalath, N. Reaction Kinetics and Characterization of Slag-Based, High Strength, ‘Just-Add-Water’ Type (One-Part) Alkali-Activated Binders. *Recent Prog. Mater.* **2022**, *4*, 6. [[CrossRef](#)]
42. Vance, K.; Aguayo, M.; Dakhane, A.; Ravikumar, D.; Jain, J.; Neithalath, N. Microstructural, Mechanical, and Durability Related Similarities in Concretes Based on OPC and Alkali-Activated Slag Binders. *Int. J. Concr. Struct. Mater.* **2014**, *8*, 289–299. [[CrossRef](#)]
43. Arora, A.; Aguayo, M.; Hansen, H.; Castro, C.; Federspiel, E.; Mobasher, B.; Neithalath, N. Microstructural packing- and rheology-based binder selection and characterization for Ultra-high Performance Concrete (UHPC). *Cem. Concr. Res.* **2018**, *103*, 179–190. [[CrossRef](#)]
44. Jiang, D.; Shi, C.; Zhang, Z. Recent progress in understanding setting and hardening of alkali-activated slag (AAS) materials. *Cem. Concr. Compos.* **2022**, *134*, 104795. [[CrossRef](#)]
45. Shi, C.; Day, R.L. A calorimetric study of early hydration of alkali-slag cements. *Cem. Concr. Res.* **1995**, *25*, 1333–1346. [[CrossRef](#)]
46. Koohestani, B.; Mokhtari, P.; Yilmaz, E.; Mahdipour, F.; Darban, A.K. Geopolymerization mechanism of binder-free mine tailings by sodium silicate. *Constr. Build. Mater.* **2021**, *268*, 121217. [[CrossRef](#)]
47. Hong, S.-Y.; Glasser, F.P. Alkali sorption by C-S-H and C-A-S-H gels: Part II. Role of alumina. *Cem. Concr. Res.* **2002**, *32*, 1101–1111. [[CrossRef](#)]
48. Fernández-Jiménez, A.; Puertas, F.; Sobrados, I.; Sanz, J. Structure of Calcium Silicate Hydrates Formed in Alkaline-Activated Slag: Influence of the Type of Alkaline Activator. *J. Am. Ceram. Soc.* **2003**, *86*, 1389–1394. [[CrossRef](#)]
49. Mueller, S.; Llewellyn, E.W.; Mader, H.M. The rheology of suspensions of solid particles. *Proc. R. Soc. A Math. Phys. Eng. Sci.* **2009**, *466*, 1201–1228. [[CrossRef](#)]
50. Santamarí, I.; Mendoza, C.I. The rheology of concentrated suspensions of arbitrarily-shaped particles. *J. Colloid Interface Sci.* **2010**, *346*, 118–126. [[CrossRef](#)]
51. Kamal, M.R.; Mutel, A. Rheological Properties of Suspensions in Newtonian and Non-Newtonian Fluids. *J. Polym. Eng.* **1985**, *5*, 293–382. [[CrossRef](#)]
52. Krieger, I.M.; Dougherty, T.J. A Mechanism for Non-Newtonian Flow in Suspensions of Rigid Spheres. *Trans. Soc. Rheol.* **1959**, *3*, 137–152. [[CrossRef](#)]
53. Brady, J.F. The rheological behavior of concentrated colloidal dispersions. *J. Chem. Phys.* **1993**, *99*, 567–581. [[CrossRef](#)]
54. Mandal, R.; Panda, S.K.; Nayak, S. Rheology of Concrete: Critical Review, recent Advancements, and future perspectives. *Constr. Build. Mater.* **2023**, *392*, 132007. [[CrossRef](#)]
55. Vance, K.; Arora, A.; Sant, G.; Neithalath, N. Rheological evaluations of interground and blended cement–limestone suspensions. *Constr. Build. Mater.* **2015**, *79*, 65–72. [[CrossRef](#)]

56. Vance, K.; Dakhane, A.; Sant, G.; Neithalath, N. Observations on the rheological response of alkali activated fly ash suspensions: The role of activator type and concentration. *Rheol. Acta* **2014**, *53*, 843–855. [[CrossRef](#)]
57. Zuo, Y.; Ye, G. Preliminary Interpretation of the Induction Period in Hydration of Sodium Hydroxide/Silicate Activated Slag. *Materials* **2020**, *13*, E4796. [[CrossRef](#)] [[PubMed](#)]
58. Khale, D.; Chaudhary, R. Mechanism of geopolymerization and factors influencing its development: A review. *J. Mater. Sci.* **2007**, *42*, 729–746. [[CrossRef](#)]
59. Provis, J.L.; van Deventer, J.S.J. Geopolymerisation kinetics. 1. In situ energy-dispersive X-ray diffractometry. *Chem. Eng. Sci.* **2007**, *62*, 2309–2317. [[CrossRef](#)]
60. Ravikumar, D.; Neithalath, N. Effects of activator characteristics on the reaction product formation in slag binders activated using alkali silicate powder and NaOH. *Cem. Concr. Compos.* **2012**, *34*, 809–818. [[CrossRef](#)]
61. Bakharev, T. Geopolymeric materials prepared using Class F fly ash and elevated temperature curing. *Cem. Concr. Res.* **2005**, *35*, 1224–1232. [[CrossRef](#)]
62. Obenaus-Emler, R.; Falah, M.; Illikainen, M. Assessment of mine tailings as precursors for alkali-activated materials for on-site applications. *Constr. Build. Mater.* **2020**, *246*, 118470. [[CrossRef](#)]
63. Chithiraputhiran, S.R. “Kinetics of Alkaline Activation of Slag and Fly ash-Slag Systems” M.S., Arizona State University, United States—Arizona. Available online: <https://www.proquest.com/docview/1269512488/abstract/3E68298DC62C47DBPQ/1> (accessed on 18 June 2023).
64. Fernández-Jiménez, A.; Zibouche, F.; Boudissa, N.; García-Lodeiro, I.; Abadlia, M.T.; Palomo, A. ‘Metakaolin-Slag-Clinker Blends.’ The Role of Na<sup>+</sup> or K<sup>+</sup> as Alkaline Activators of Ternary Blends. *J. Am. Ceram. Soc.* **2013**, *96*, 1991–1998. [[CrossRef](#)]

**Disclaimer/Publisher’s Note:** The statements, opinions and data contained in all publications are solely those of the individual author(s) and contributor(s) and not of MDPI and/or the editor(s). MDPI and/or the editor(s) disclaim responsibility for any injury to people or property resulting from any ideas, methods, instructions or products referred to in the content.